buildings

MDPI

Article

Early-Age Shrinkage Stress of Alkali-Activated Cement-Free Mortar Using Shrinkage Reducing Agent and Expansive Additive

Seok-ho Yoon [1], Sung-rok Oh [2], Ji-young Kim [3] and Sung Choi [1,*]

[1] Department of Civil Engineering, Kyungdong University, 27, Gyeongdongdaehak-ro, Yangju-si 11458, Gyeonggi-do, Republic of Korea; shyoon@kduniv.ac.kr
[2] Department of Civil Engineering, Semyung University, 65, Semyeong-ro, Jecheon-si 27136, Chungcheongbuk-do, Republic of Korea; cgdbs02@nate.com
[3] Smart Hi-Tech Group, Samsung E&A, 26, Sangil-ro 6 gil, Gangdong-gu, Seoul 05288, Republic of Korea; jy0421.kim@samsung.com
* Correspondence: csomy1113@kduniv.ac.kr

Abstract: Cement-free concrete has a superior physical performance, such as in its strength and durability, compared to OPC concrete; however, it has the disadvantage of large shrinkage. Large shrinkage can cause cracks due to shrinkage stress in the long term. In this study, a shrinkage reducing agent (SRA) was used to reduce the shrinkage of cement-free mortar; its content was increased from 0.0 to 1.5%. For an SRA content of 1.0%, a calcium sulfoaluminate (CSA) expansive additive (EA) (2.5, 5.0, and 7.5%) was added. To calculate the shrinkage stress of cement-free mortar using the SRA and EA, the compressive strength, elastic modulus, and total and autogenous shrinkage were measured. The unit shrinkage stress of cement-free mortar was obtained by multiplying the elastic modulus by the length change and accumulated to obtain the shrinkage stress acting on the mortar according to the age. The shrinkage stress of cement-free mortar showed different tendencies as the age increased. At early ages, the shrinkage rate of the mortar occupied a large proportion of the shrinkage stress. In the long term, the shrinkage stress was significantly affected by the elastic modulus. As a result, SRA was found to be effective in reducing the shrinkage stress by decreasing both the elastic modulus and shrinkage. However, EA increased the shrinkage stress over the long term due to an increase in the elastic modulus even though it compensated for early-ages shrinkage.

Keywords: cement-free mortar; CSA expansive additive; elastic modulus; shrinkage reducing agent; shrinkage stress

Citation: Yoon, S.-h.; Oh, S.-r.; Kim, J.-y.; Choi, S. Early-Age Shrinkage Stress of Alkali-Activated Cement-Free Mortar Using Shrinkage Reducing Agent and Expansive Additive. *Buildings* **2024**, *14*, 1852. https://doi.org/10.3390/buildings14061852

Academic Editors: Peiyu Yan, Yao Luan and Chunsheng Zhou

Received: 14 February 2024
Revised: 20 May 2024
Accepted: 31 May 2024
Published: 18 June 2024

1. Introduction

Cement, the main material for developing concrete performance, emits a large amount of carbon dioxide (CO_2) during its production process. Thus, as part of efforts to realize carbon neutrality, various studies have been conducted to reduce CO_2 emissions in the cement industry [1–7]. Among them, the most actively researched topic is cement-free binder, which does not use cement at all. The materials typically used in the research on cement-free binder are blast-furnace slag (BFS) and fly ash (FA), which are industrial by-products. By simultaneously using these materials and an appropriate amount of alkali activator to induce the reaction, a similar performance to ordinary Portland cement (OPC)-based mortar and concrete can be achieved. In this way, cement-free binder using industrial by-products is an eco-friendly material that can replace existing cement, and its applicability has been verified through many studies [8–11].

Cement-free mortar has the advantages of high strength at early ages, excellent chloride resistance, chemical resistance, and durability [12]. However, cement-free mortar tends to undergo a large shrinkage process, which also has a problem of increasing the risk

of cracking [13]. The shrinkage of cement-free mortar mostly occurs at early ages. Over the long term, the shrinkage increment decreases; however, it continuously occurs and increases the risk of cracking. To address these problems, studies have been conducted on the shrinkage characteristics of cement-free mortar. Cartwright et al. [14] prepared alkali-activated slag (AAS) mortar using various activators and measured autogenous and drying shrinkage. They found that AAS causes up to six times higher shrinkage than OPC. Collins et al. [15] reported that higher shrinkage occurs to cement-free mortar because it is subjected to higher capillary stress as its pore size is smaller than that of OPC. The cracks caused by the shrinkage of cement-free mortar are considered to be the most serious problem in applying the mortar to structures [13,16]. Cement-free binders have excellent physical properties and high durability; however, this applies when there is no crack in the matrix of the cement-free mortar and concrete. The application of cement-free binders to structures can result in shrinkage leading to cracks depending on the constraints and curing conditions. The generated shrinkage cracking may lead to uncertainty about the durability of cement-free mortar over the long term [17,18].

Various methods can be applied to control shrinkage cracking. Among these, shrinkage reducing agents (SRAs) and expansive additives (EAs) are commonly used as a material approach. In the study of Abolfathi et al. [19], the polypropylene (PP), steel fiber (SF), and hexylene glycol-based SRA were used for mitigating the shrinkage of alkali-activated slag and fly ash (AASF) mortars incorporating a recycled fine aggregate (RFA), and its characteristics were analyzed. As a result, although the initial compressive strength of AASF mortar incorporating SRA was reduced, a similar level of strength to the reference specimen was obtained at 28 days; in addition, the free and restrained shrinkage were mitigated compared to the specimens incorporating PP and SF. Al Makhadmeh and Soliman [20] established the mechanisms of SRA by conducting research on the behavior of SRA and its interaction with the pore solution and systems of AAS. The high shrinkage of AAS systems is due to the high ratio of mesopores and the formation of silica gel with a high tendency to shrink. According to the results, SRA delayed the hydration and extended the setting time by reducing the dissolution affinity of ions, and reduced shrinkage caused by C-A-S-H syneresis by lowering the degree of the polymerization of C-A-S-H, the main hydrate. Xu et al. [21] used a MgO-based expansion agent (MEA) for mitigating the shrinkage of alkali-activated blast furnace slag–copper slag (AAS-CS). The addition of MEA exerted the filling effect and shrinkage-compensating effect by promoting the formation of hydrotalcite (Ht), an expansive hydrate, and the lowest shrinkage rate and highest compressive strength appeared when 4.0 wt% of MEA was added. Choi et al. [22] used CSA EA to compensate for the shrinkage of cement-free mortar and reported that the shrinkage stress of the mortar was not significantly reduced because it increased the elastic modulus as it reduced the shrinkage of the mortar.

In summarizing the existing research results, it can be seen that SRAs do not affect the mineralogical composition of cement-free mortar and could reduce shrinkage by altering the pore structure and surface tension depression [23]; however, they can also reduce the compressive strength by affecting the hydration reaction. On the other hand, EAs not only the reduce shrinkage of cement-free mortar by compensating for it with the expansion effect of hydrates, but they also have the effect of increasing the compressive strength or elastic modulus. When material supplementation is used to reduce the shrinkage of cement-free mortar, the factors that affect the characteristics of cement-free mortar as well as shrinkage must be comprehensively investigated, and technologies must be applied that can accurately predict the stress caused by shrinkage and reduce shrinkage in a timely manner. In this study, an SRA and EA were used to reduce the shrinkage of cement-free mortar, and the shrinkage stress acting on the mortar was analyzed. To calculate the shrinkage stress of cement-free mortar with an SRA and EA, the total and autogenous shrinkages were measured for 150 days, and the elastic modulus was measured at early ages (1 and 2 days of age) and at larger ages (28 and 91 days). In addition, a model equation for the elastic modulus of cement-free mortar according to the SRA and EA contents was

established by applying the experimental values of the elastic modulus by age to the ACI 209 model equation. The use of the shrinkage of cement-free mortar and the model equation makes it possible to obtain the shrinkage stress of the mortar per unit time (unit shrinkage stress), and the cumulative shrinkage stress acting on the mortar at any age can be obtained by accumulating the unit shrinkage stress. The shrinkage stress of cement-free mortar varied depending on the SRA and EA contents used for shrinkage reduction; this was analyzed at an early age (2 days) and a later age (150 days).

2. Materials and Methods

2.1. Materials and Mixture Proportions of Cement-Free Mortar

Table 1 shows the physical properties and chemical compositions of the binders used in cement-free mortar (ground granulated blast furnace slag (GGBFS) and FA), admixtures used for shrinkage reduction (SRA and EA), and alkali-activator (A-Act.). GGBFS used as a binder satisfies the type 3 criteria of KS F 2563 [24], and FA meets the type 2 criteria of KS F 5405 [25].

Table 1. Physical properties and chemical composition of materials used.

Type	Density (kg/m^3)	Blaine (m^2/kg)	CaO (%)	SiO_2 (%)	Al_2O_3 (%)	Fe_2O_3 (%)	SO_3 (%)	MgO (%)	K_2O (%)	Na_2O (%)	L.O.I. (%)
GGBFS	2908	468	43.4	34.6	14.3	0.6	5.0	5.1	0.5	0.2	−0.2
FA	2203	322	3.5	56.8	22.8	6.9	0.5	1.8	1.1	0.8	2.4
SRA	3160	-	1.4	29.0	0.2	0.1	-	0.1	-	-	69.2
EA	2862	375	36.3	30.1	24.5	1.6	5.1	1.3	0.6	0.3	0.3
A-Act.	1026	-	-	46.3	-	-	-	-	-	50.5	-

The GGBFS was produced from POSCO steelworks (Pohang, Republic of Korea) and its major chemical components were CaO (43.4%), SiO_2 (34.6%), and Al_2O_3 (14.3%). The basicity coefficient (K_b = (CaO + MgO)/(SiO_2 + Al_2O_3)) of the GGBFS was 0.99, which was close to the neutral value for ideal alkali activation (1.0). Its hydration modulus (HM = (CaO + MgO + Al_2O_3)/SiO_2) was 1.82, which is higher than 1.4, the value for an excellent hydration reaction. The FA was a product obtained by processing the industrial by-products generated from KOREA MIDLAND POWER Co. (Boryeong, Republic of Korea). Its main chemical components were SiO_2 (56.8%), Al_2O_3 (22.8%), and Fe_2O_3 (6.9%) with a M_2O (K_2O + Na_2O) content of 1.9%. The EA was produced in Japan and was based on calcium sulfoaluminate (CSA); it contained CaO (36.7%), SiO_2 (30.4%), and Al_2O_3 (24.7%). The density and fineness of EA were 2.90 g/cm^3 and 3100 cm^2/g, respectively. The SRA was a white powder and was composed of SiO_2 and organic components. The SRA used in this study was glycols-based. The density and ash content of SRA were 3.16 g/cm^3 and 40%, respectively. The A-Act was a white water-soluble powder, and its main chemical components were SiO_2 and Na_2O (96.8%). The alkali activator was in the form of a white powder with a molar ratio of 0.95. In addition, alkali activators are manufactured separately by adjusting the chemical components. The ratio between SiO_2 and Na_2O was 0.92. Figure 1 shows the particle size distribution curve of the fine aggregate. The fine aggregate used in the mortar was river sand, which had a density of 2.51 g/cm^3, a water absorption of 1.09%, and a fineness modulus of 2.82.

Table 2 summarizes the mix proportions of cement-free mortar. A two-component binder in which GGBFS and FA were mixed at a ratio of 7:3 was used, and the A-Act content was 24% per unit of water content. Since the GGBFS:FA was fixed to 7:3 in the previous study [22] which used EA only, for intercomparison with it, the mix ratio of binder was determined to be the same as the previous study [22]. The water-to-binder (W/B) ratio was 0.451 and the sand-to-binder (S/B) ratio was 1.2.

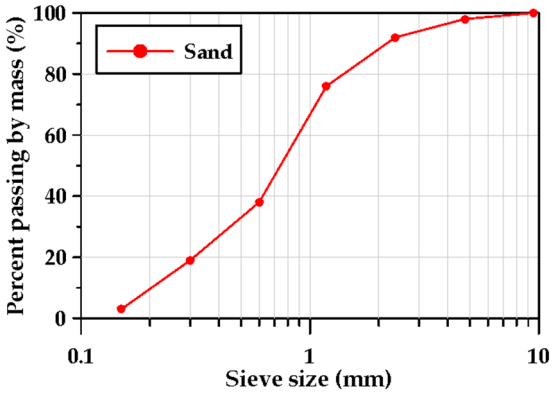

Figure 1. Particle size distribution curve of fine aggregates.

Table 2. Mix proportions of the cement-free mortar.

Type	Water (g)	Binder (g)	Activator (g)	Sand (g)	SRA (g)	EA (g)
S0.0	451	1000	108	1200	0	0
S0.5	451	1000	108	1200	2.26	0
S1.0	451	1000	108	1200	4.51	0
S1.5	451	1000	108	1200	6.77	0
S1E2.5	451	1000	108	1200	4.51	25
S1E5.0	451	1000	108	1200	4.51	50
S1E7.5	451	1000	108	1200	4.51	75

The SRA contents were 0.5, 1.0, and 1.5% per unit of water content. For the cement-free mortar that used both an SRA and EA, the SRA content was 1.0% and the EA content was 2.5, 5.0, and 7.5% compared to the unit binder content (since the dosage rate of EA had been 0, 2.5, 5.0, and 7.5% in the previous study [22], for association with it, the dosage rate of EA started from 2.5%). In total, seven types of cement-free mortar were prepared.

To prepare the cement-free mortar, the basic binder, A-Act, SRA, and EA were placed in a test container and dry-mixed for 30 s. The weighed water was added to the mixture and mixing was performed at 150 rpm for ten minutes to create a paste. Finally, the weighed fine aggregate was added, and mixing was performed at 300 rpm for 90 s.

2.2. Test Methods

2.2.1. Compressive Strength Test

Figure 2 shows the compressive strength test. The compressive strength test was conducted in accordance with ASTM C 39/M (2018) [26]. The specimens for this test were prepared using a cylindrical specimen mold with a diameter of 100 mm and height of 200 mm. The test was conducted at 1, 2, 28, and 91 days of age. The specimens were cured in a constant temperature and humidity chamber at a temperature of 23 ± 2 °C and a relative humidity of 90 ± 2% for 1 day, and then water-cured at same temperature until the ages of the compressive strength measurement. Before testing, the specimens were dried for 2 h to avoid the influence of pore water pressure. The test results of the three specimens were averaged and used as the compressive strength at each age.

Figure 2. The compressive strength test.

2.2.2. Modulus of Elasticity Test

Figure 3 shows the elastic modulus test. The elastic modulus test was conducted in accordance with ASTM C 469M-14 [27]. Specimens for this test were cylindrical with a diameter of 100 mm and a height of 200 mm. The test was conducted at 1, 2, 28, and 91 days of age. For the elastic modulus measurement, two strain gauges were installed on the side of each specimen. The test was conducted after checking the normal operation of the gauges by applying a load twice. After loading up to 40% of the ultimate load at a rate of 0.25 MPa/s, the elastic modulus was calculated through the regression of the deformation under the load using an interpolation method. The measurements of the three specimens were averaged and used as the elastic modulus. The specimens were cured in a constant temperature and humidity chamber at a temperature of 23 ± 2 °C and a relative humidity of 90 ± 2% for 1 day, and then water-cured at the same temperature until the ages of the modulus of elasticity measurement.

(**a**) (**b**) (**c**)

Figure 3. The elastic modulus test: (**a**) strain gauge; (**b**) test specimen; and (**c**) overall setup for measurement.

2.2.3. Shrinkage Test

Figure 4 shows the specimen for conducting the shrinkage test. To measure the length change rate of the mortar, 100 × 100 × 400 mm prismatic specimens were prepared. In the center of each specimen, an embedded gauge (PMFL-50-2LT, Tokyo Sokki Kenkyujo Co., Ltd., Tokyo, Japan) for the length change and a temperature sensor (Thermocouple t type, Tokyo Sokki Kenkyujo Co., Ltd., Tokyo, Japan) were installed. Before pouring the mortar, Teflon sheets and polystyrene boards were installed on the inner surface of the mold to minimize the friction between the mold and the constraint in the longitudinal direction. After pouring the mortar, polyester films were installed on the surface to prevent the evaporation and absorption of moisture on the surface of the specimen. The cement-free mortar specimens were demolded after one day of curing. For measuring the autogenous shrinkage, the specimens were sealed with polyester films to control drying. For measuring the total shrinkage, which is the sum of drying and autogenous shrinkage, the specimens

were not sealed after demolding. The length change of the cement-free mortar was measured in a constant temperature and humidity chamber (temperature 20 °C and relative humidity 60%). The length change rate data were received every 30 min and the total measurement period was 150 days.

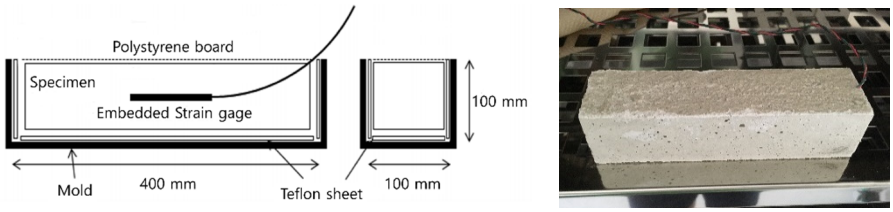

(**a**) (**b**)

Figure 4. The specimen for conducting shrinkage test: (**a**) schematic and (**b**) photograph.

3. Results

3.1. Compressive Strength

Table 3 shows the compressive strengths of the cement-free mortars that used the SRA and EA, which were used for shrinkage reduction. The binder of the cement-free mortar shows a fast reaction at the beginning due to the stimulation of the A-Act, and the strength rapidly increases at early ages [28,29].

Table 3. Compressive strength of cement-free mortar.

Age (Day)	S0.0 (MPa)	S0.5 (MPa)	S1.0 (MPa)	S1.5 (MPa)	S1E2.5 (MPa)	S1E5.0 (MPa)	S1E7.5 (MPa)
1	2.88	2.27	2.17	2.12	3.90	4.28	4.57
2	34.45	27.74	26.02	27.85	28.95	33.28	33.45
28	45.39	38.65	37.74	37.57	40.89	46.13	48.77
91	52.35	47.26	42.10	41.65	43.58	50.03	50.90

Meanwhile, the reaction rate of this hydration mechanism varies depending on the admixture used [30]. On day 1, the compressive strengths of the cement-free mortars that used the SRA were lower than that of S0.0, which did not use the SRA; the compressive strengths decreased as the content of the SRA increased. Bílek et al. [31] reported that an increase in the content of the SRA may intensify this strength reduction phenomenon because the SRA decreases the surface tension of mixing water to reduce the drying shrinkage, thereby delaying the ionic reaction of the A-Act dissolved in the mixing water and the alkali stimulation of the binder. In addition, Nguyen et al. [32] demonstrated that the reduction in the hydration reaction caused by an SRA may last for an extended period. In the experimental results of the present study, the cement-free mortar using the SRA showed lower compressive strengths at 28 and 91 days of age than S0.0.

The cement-free mortar using the SRA and EA exhibited higher compressive strengths than S0.0 on day 1, but its strengths were lower than that of S0.0 after day 2. The compressive strengths of the cement-free mortars using the EA increased on day 1 due to the expansion effect of the EA. The EA forms ettringite as a hydrate mainly at the early ages, which increases the compressive strength and has the effect of reducing shrinkage. Since this expansion effect of the EA was significant from days 1 to 2 and decreases afterwards, the strength reduction phenomenon of the EA occurred over the long term [33].

3.2. Modulus of Elasticity

Figure 5 shows the experimental values of the elastic modulus of the cement-free mortar using the SRA and EA and the prediction curve by the ACI 209 model equation [34].

The elastic modulus of the cement-free mortar using SRA showed no significant difference from that of S0.0 at day 1, but it was lower over the long term (after 28 days). This is because the cement-free mortar using the SRA has many pores [35,36]. On the other hand, the elastic modulus of the cement-free mortar using the SRA and EA was higher than that of S0.0 because the hydrates of the EA, which are expansive substances, filled the pores of the mortar and densified its inside, leading to the improved pore structure by the hydrates of the EA along with the generated hydrates of the mortar [37].

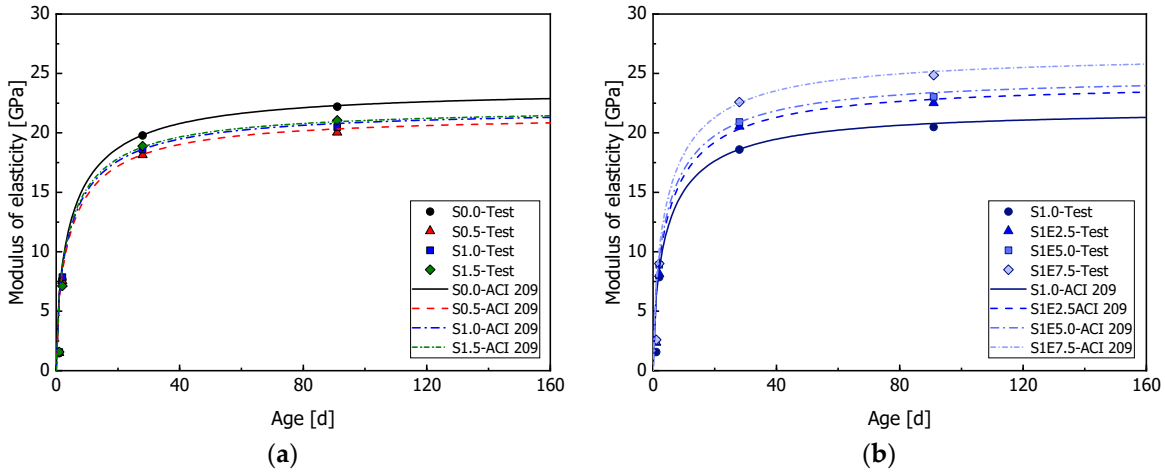

Figure 5. Comparison of the elastic modulus from the experimental values and the ACI 209 model equation: (**a**) usage of SRA and (**b**) usage of SRA and EA.

To analyze the change in the elastic modulus caused by the SRA and EA, a prediction curve was derived by applying the experimental values of the elastic modulus to the ACI 209 model equation which can predict the influence of the material used on the elastic modulus at early ages and at long ages, as follows:

$$E_{cmt} = E_{cm28}\sqrt{\frac{t}{a+bt}} \quad (1)$$

where E_{cmt} denotes the elastic modulus of cement-free mortar at age t, E_{cm28} denotes the elastic modulus at 28 days of age, and a and b denote the material constants.

Table 4 summarizes the material constants of the elastic modulus of the cement-free mortar using SRA and EA. The R^2 (coefficient of determination) between the experimental values and the ACI 209 model equation ranged from 0.915 to 0.949. Based on S0.0 with no admixture (SRA or EA), the change in the material constants of the elastic modulus caused by the use of the admixtures was analyzed. a is the constant for the maximum value of the elastic modulus. When the tendency of a was analyzed according to the contents of the admixtures used (SRA and EA), a decreased as the content of the SRA increased, but increased as the content of the EA increased when both the SRA and EA were mixed. This is because the long-term elastic modulus was high when the EA was used. b is the rate of change of the elastic modulus, which increases with age. b showed a tendency to increase as the content of the SRA increased. When both the SRA and EA were mixed, b showed a tendency to decrease as the content of the EA increased. The material constants a and b obtained by applying the elastic modulus of the cement-free mortar using the SRA and EA to the ACI 209 model equation can be used to predict the elastic modulus of the mortar at any age.

Table 4. Material constants and coefficient of determination of the elastic modulus of cement-free mortar.

Type	S0.0	S0.5	S1.0	S1.5	S1E2.5	S1E5.0	S1E7.5
a	8.496	8.122	8.020	7.831	8.456	8.735	9.016
b	0.697	0.710	0.714	0.720	0.698	0.688	0.678
R^2	0.915	0.918	0.919	0.920	0.945	0.949	0.945

3.3. Shrinkage

Figure 6 shows the total shrinkage (ε_{tsh}) and autogenous shrinkage (ε_{ash}) of cement-free mortar depending on the contents of the SRA and EA. Table 5 summarizes the shrinkage test results of the cement-free mortar using the SRA and EA at day 1, 2, and 150.

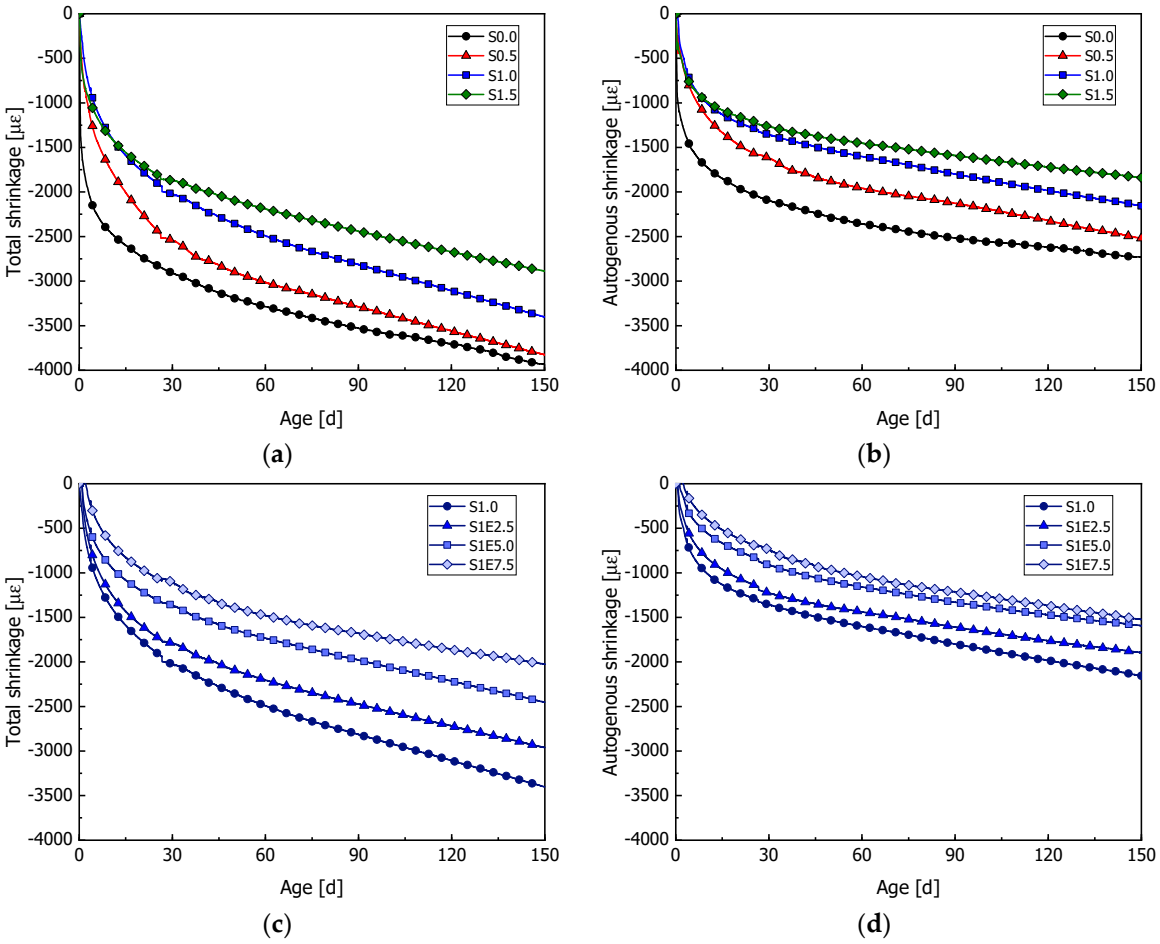

Figure 6. Shrinkage curves of cement-free mortar: (**a**) total shrinkage (SRA); (**b**) autogenous shrinkage (SRA); (**c**) total shrinkage (S1.0 + EA); and (**d**) autogenous shrinkage (S1.0 + EA).

For S0.0 without an SRA or EA, the total shrinkage was measured to be −3932 με on day 150. The total shrinkage was 41.6% (−1637 με) on day 1 and 47.1% (−1853 με) on day 2, indicating that significant shrinkage occurred on these days. At early ages, when significant shrinkage occurs, the elastic modulus increases, causing significant changes in the early-ages shrinkage stress that acts on cement-free mortar. The total shrinkage of the cement-free mortar using the SRA, however, was lower than that of S0.0 at early ages (0 to 2 days). The total shrinkage reduction rate increased as the content of the SRA increased. The total shrinkage of S1.5 with the highest content of the SRA was approximately 19.9% of that of S0.0 at day 1. The total shrinkage of S1.0 was also approximately 40.9% of that of

S0.0 at day 1. The total shrinkage for the case of mixing the EA with S1.0 was even lower than that of S1.0 at day 1. Particularly, S1E7.5, with the highest EA content, showed an expansion of 7 με. As the content of the SRA and EA increased, the total shrinkage at day 150 decreased, but the total shrinkage reduction rate was lower compared to day 1.

Table 5. ε_{ash} and $\varepsilon_{tsh} - \varepsilon_{ash}$ of cement-free mortar over 150 days.

Type	ε_{tsh} (με)			ε_{ash} (με)			$\varepsilon_{tsh} - \varepsilon_{ash}$ (με)		
	1 d	**2 d**	**150 d**	**1 d**	**2 d**	**150 d**	**1 d**	**2 d**	**150 d**
S0.0	−1637	−1853	−3932	−1096	−1237	−2728	−541	−616	−1204
S0.5	−822	−969	−3826	−437	−626	−2518	−385	−343	−1308
S1.0	−670	−838	−3401	−424	−554	−2154	−246	−284	−1247
S1.5	−326	−621	−2887	−264	−443	−1839	−62	−178	−1048
S1E2.5	−365	−485	−2960	−184	−335	−1896	−181	−150	−1064
S1E5.0	−109	−344	−2452	+11	−119	−1594	−120	−225	−858
S1E7.5	+7	−7	−2024	+29	+24	−1523	−22	−31	−501

Cement-free mortar also exhibited significant autogenous shrinkage at early ages. The autogenous shrinkage curve of S0.0 according to the age showed a tendency similar to that of the total shrinkage. The autogenous shrinkage at day 150 was 40.2% on day 1 and 45.3% on day 2. When the SRA was used, the autogenous shrinkage reduced. The autogenous shrinkage of S1.0 was approximately 38.7% of that of S0.0 on day 1 and the reduction rate was similar to that of the total shrinkage. When the EA was added to S1.0, the autogenous shrinkage reduced. Depending on the content of the EA, expansion was also observed. The cement-free mortar using the SRA and EA showed a reduction in autogenous shrinkage even at day 150, at which its reduction rate, compared to S1.0, showed a tendency similar to that of the total shrinkage reduction rate. In this instance, the difference between the autogenous and total shrinkage reduction rate was found to be less than 7.5%. The total shrinkage is the sum of the autogenous and drying shrinkage, and the SRA and EA, which are used to reduce the shrinkage of cement-free mortar, have the effect of reducing the total shrinkage [38–40].

To validate the shrinkage results obtained in this study, previous studies conducted under a similar topic were investigated. The total shrinkage at 150 days in this study was in the range of 2000–4000 με and this result was similar to [23], which had a similar range using the SRA up to 2%. In addition, the drying shrinkage at 56 days using the SRA and EA were approximately 1000 με and in the range of 500–1000 με, respectively, and these results were similar to [33]. It can be confirmed that although the exact results were slightly different due to the different types of the SRA and EA and mixture proportions, the range of results were similar between this study and previous studies. In a previous study, AAM mortar with the CSA EA showed shrinkage reduction at an early age due to the expansion characteristic of the CSA EA, but there was no further reduction after 3 days [22]. In this study, shrinkage reduction occurred for 150 days when the EA and SRA were used together, which we believe is due to the influence of the SRA.

3.4. Stress of Shrinkage (2 Days)

For cement-free mortar, significant shrinkage occurs at early ages. Such shrinkage may cause stress depending on the constraint conditions, and this stress may cause cracking at early ages when the strength of cement-free mortar is low [41]. The use of admixtures, such as the SRA and EA, can reduce the shrinkage of cement-free mortar. However, changes in the elastic modulus over time must be considered because the shrinkage stress is affected by both the shrinkage rate and the elastic modulus. Since both the shrinkage and elastic modulus of cement-free mortar change over time, the shrinkage stress ($f_{(sh,t+\Delta t)}$) is

calculated by adding the stress caused by shrinkage per unit of time (Δf_{sh}) to the shrinkage stress acting on the cement-free mortar ($f_{(sh,t)}$) [22,42], as follows:

$$f_{(sh,t+\Delta t)} = f_{(sh,t)} + \Delta f_{sh} \quad (2)$$

$$\Delta f_{sh} = E \times \Delta \varepsilon_{sh} \quad (3)$$

Figure 7 shows the unit shrinkage stress and cumulative shrinkage stress of cement-free mortar until day 2. The unit shrinkage stress (Δf_{sh}) is the shrinkage stress calculated per unit of time and is obtained by multiplying the shrinkage rate, which varies every 30 min, by the elastic modulus. The cumulative shrinkage stress is the shrinkage stress acting on the cement-free mortar at time t and is obtained by adding the unit shrinkage stress to the shrinkage stress of the cement-free mortar.

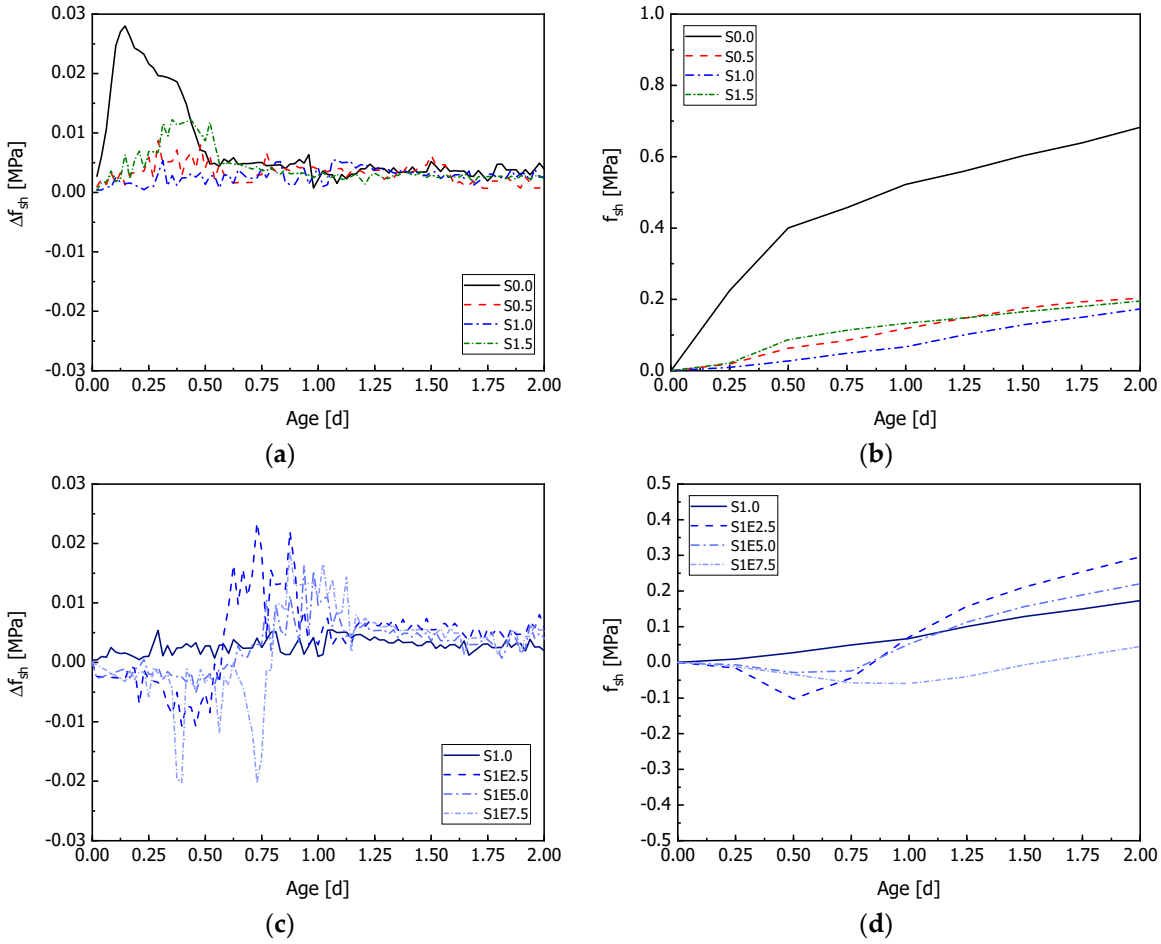

Figure 7. Shrinkage stress over 2 days caused by the shrinkage of cement-free mortar: (**a**) unit shrinkage stress (Δt: 30 min) according to usage of SRA; (**b**) cumulative shrinkage stress according to usage of SRA; (**c**) unit shrinkage stress (Δt: 30 min) according to usage of S1.0 and EA; and (**d**) cumulative shrinkage stress according to usage of S1.0 and EA.

The unit shrinkage stress of S0.0 increased from 0 to 0.146 days (3.5 h). The shrinkage stress reached a maximum of 0.028 MPa and then decreased until 0.5 days. Until 0.5 days, the unit shrinkage stress was high because the total shrinkage rapidly increased even though the elastic modulus was not yet large. However, after 0.5 days, the low unit shrinkage stress was maintained. The average unit shrinkage stress during the period from 0.5 to 2 days was approximately 0.004 MPa. Thus, the cumulative shrinkage stress of S0.0 increased until 0.5 days, and its increment decreased after 0.5 days.

The unit shrinkage stress of the cement-free mortar using the SRA was not large until 0.5 days. As the content of the SRA increased, the maximum unit shrinkage stress showed a tendency to decrease. This is because the shrinkage of the cement-free mortar using SRA was not high at the beginning and its elastic modulus was also low compared to that of S0.0. The unit shrinkage stress of the cement-free mortar using the SRA reached its peak at 0.25 to 0.31 days. The occurrence of the maximum unit shrinkage stress was delayed compared to S0.0 because the increase in the elastic modulus was delayed even though the cement-free mortar using the SRA also had the same tendency to exhibit significant shrinkage at the beginning.

The shrinkage of the cement-free mortar using the SRA and EA at early ages was further reduced and expansion occurred for a certain period. The unit shrinkage stress indicated that the expansion stress occurred for all specimens at the beginning and then shrinkage stress occurred. The duration of the expansion stress was shortest (11 h) for S1E2.5, which had the lowest content of the EA, and longest (16.5 h) for S1E7.5. The maximum value of the expansion stress was not proportional to the content of the EA because the time point at which expansion occurred and the time point at which the elastic modulus increased were different depending on the specimens. The cumulative shrinkage stress of S1E2.5 and S1E5.0 on day 2 exhibited larger values than S1.0 without the EA. This is because the elastic modulus was increased by the EA.

3.5. Stress of Shrinkage (150 Days)

The shrinkage stress of cement-free mortar is affected by the shrinkage rate and elastic modulus. As outlined in Section 3.4, the shrinkage significantly changes and has a large impact on shrinkage stress at early ages; however the influence of the elastic modulus increases as the age increases because the rate of the change of shrinkage decreases and the elastic modulus increases with time. Figure 8 shows the unit shrinkage stress and cumulative shrinkage stress of cement-free mortar until day 150.

The unit shrinkage stress results show that the unit shrinkage stress significantly varied until day 20. This is because the shrinkage measured by the data logger before day 20 had deviations of the unit time. After day 20, curves with a certain tendency were observed because the shrinkage of cement-free mortar did not significantly increase and thus the rate of the change of shrinkage per unit of time was small. In the unit shrinkage stress results over 150 days, S0.0 showed the highest shrinkage stress and the unit shrinkage stress of the cement-free mortar using the SRA decreased. The unit shrinkage stress shows a tendency to slightly increase after 20 days because the elastic modulus is large even though the shrinkage increment is small. At day 150, S0.0 showed the highest unit shrinkage stress (0.002397 MPa) and S1.5 showed the lowest unit shrinkage stress (0.001344 MPa).

The cumulative shrinkage stress results show that the shrinkage stress of S0.0 significantly increased at the beginning, and the cumulative shrinkage stresses rapidly increased until later ages. Meanwhile, the cumulative shrinkage stresses of the cement-free mortars using the SRA increased gently compared to that of S0.0. At day 150, S0.0 showed the highest cumulative shrinkage stress of 4.306 MPa. As the content of the SRA increased, the cumulative shrinkage stress decreased at day 150. Compared to S0.0, the cumulative shrinkage stress decreased by 40.7%, 42.4%, and 56.6% for S0.5, S1.0, and S1.5, respectively.

The unit shrinkage stress of the cement-free mortar made by adding the EA to S1.0 also significantly fluctuated until day 20, and the expansion section caused by the EA occurred at the beginning. The EA decreased the shrinkage of the cement-free mortar; however, a high unit shrinkage stress compared to S1.0 was observed over the long term due to the increase in the elastic modulus. When the unit shrinkage stress was compared in terms of the content of the EA, S1E2.5 exhibited the highest unit shrinkage stress (3.824 MPa) at day 150 followed by S1E5.0 (3.323 MPa) and S1E7.5 (3.157 MPa), but there was no significant difference in the unit shrinkage stress.

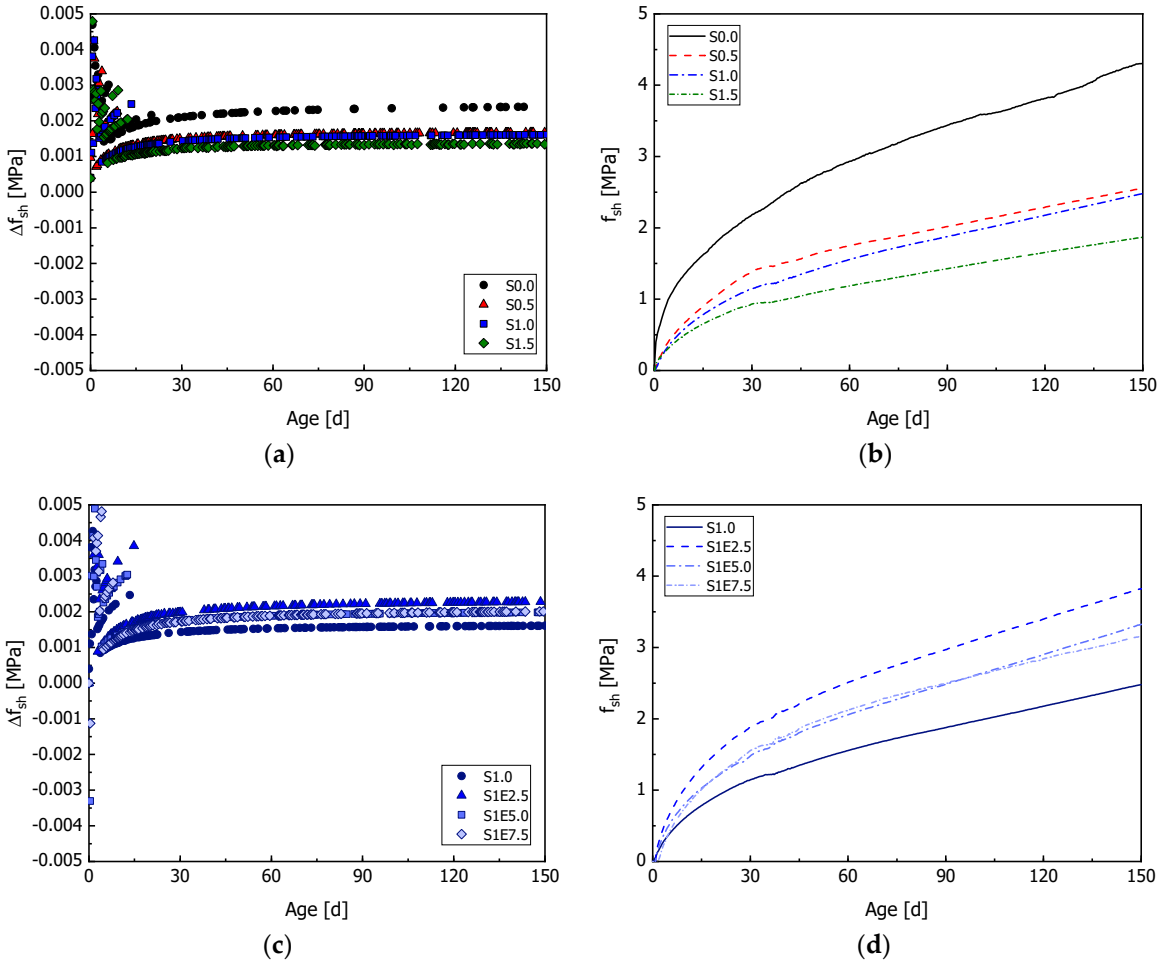

Figure 8. Shrinkage stress over 150 days caused by the shrinkage of cement-free mortar: (**a**) unit shrinkage stress (Δ*t*: 30 min) according to usage of SRA; (**b**) cumulative shrinkage stress according to usage of SRA; (**c**) unit shrinkage stress (Δ*t*: 30 min) according to usage of S1.0 and EA; and (**d**) cumulative shrinkage stress according to usage of S1.0 and EA.

4. Conclusions

An SRA and EA were used to reduce the shrinkage of cement-free mortar; the shrinkage stress was calculated using the compressive strength, elastic modulus, and shrinkage test results, and the shrinkage stress acting on the cement-free mortar at early ages and over the long term was analyzed. We draw the following conclusions from our results.

1. Using an SRA only, the compressive strengths decreased as the content of the SRA increased due to the low surface tension of the mixing water and a delay in the hydration reaction. When using both an SRA and EA, the initial compressive strengths were higher than those of S0.0 due to the expansion effect; however, this phenomenon was not continued over the long term.
2. At early ages (2 days), the unit shrinkage stress decreased, and the occurrence of the maximum unit shrinkage stress was delayed when using the SRA since it had the low elastic modulus compared to the S0.0 specimens. Meanwhile, the expansion occurred when using both the SRA and EA and the duration of the expansion increased as the EA content increased. In addition, the cumulative shrinkage stress was larger than S1.0 due to the increase in the elastic modulus by the EA.
3. At later ages (150 days), the influence of the elastic modulus increased the cumulative shrinkage stress. As the SRA content increased, the cumulative shrinkage stress decreased due to the low shrinkage rate and low elastic modulus. Meanwhile, the

cumulative shrinkage stress of the specimens incorporating the EA increased despite the reduced shrinkage rate due to the increase in the elastic modulus.

The use of the shrinkage stress monitoring technique based on the shrinkage and elastic modulus of mortar makes it possible to predict the long-term shrinkage stress of cement-free mortar and quantitatively evaluate the reduction in the shrinkage stress by expansive materials that are used for shrinkage reduction. In addition, the influence of shrinkage on the mechanical performance of structures can be evaluated through research on the shrinkage stress of structures that use cement-free binders according to constraint and curing conditions. In further research, for better understanding the microstructure change at early ages, the correlation between the shrinkage stress and microstructure of cement-free mortar should be investigated through X-ray diffraction (XRD), mercury intrusion porosimetry (MIP), gas pycnometry (GP), and scanning electron microscopy (SEM).

Author Contributions: Conceptualization, S.C., S.-h.Y. and S.-r.O.; investigation, S.-r.O. and J.-y.K.; resources, S.-h.Y.; writing—original draft, S.-h.Y. and S.-r.O.; writing—review and editing, S.-r.O. and J.-y.K.; supervision, S.-h.Y.; project administration, S.C.; funding acquisition, S.C. All authors have read and agreed to the published version of the manuscript.

Funding: This research received no external funding.

Data Availability Statement: Data are contained within the article.

Acknowledgments: This research was supported by a grant (22CTAP-C163834-02) from the Construction Technology Research Program funded by the Ministry of Land, Infrastructure, and Transport of the Korean government.

Conflicts of Interest: The authors declare no conflicts of interest.

References

1. Miller, S.A.; John, V.M.; Pacca, S.A.; Horvath, A. Carbon dioxide reduction potential in the global cement industry by 2050. *Cem. Concr. Res.* **2018**, *114*, 115–124. [CrossRef]
2. Barcelo, L.; Kline, J.; Walenta, G.; Gartner, E. Cement and carbon emissions. *Mater. Struct.* **2014**, *47*, 1055–1065. [CrossRef]
3. Hasanbeigi, A.; Price, L.; Lin, E. Emerging energy-efficiency and CO_2 emission-reduction technologies for cement and concrete production: A technical review. *Renew. Sustain. Energy Rev.* **2012**, *16*, 6220–6238. [CrossRef]
4. Das, S.; Saha, P.; Jena, S.P.; Panda, P. Geopolymer concrete: Sustainable green concrete for reduced greenhouse gas emission–A review. *Mater. Today Proc.* **2022**, *60*, 62–71. [CrossRef]
5. Yang, K.H.; Jung, Y.B.; Cho, M.S.; Tae, S.H. Effect of supplementary cementitious materials on reduction of CO_2 emissions from concrete. *J. Clean. Prod.* **2015**, *103*, 774–783. [CrossRef]
6. Wang, X.Y.; Lee, H.S. Effect of global warming on the proportional design of low CO_2 slag-blended concrete. *Constr. Build. Mater.* **2019**, *225*, 1140–1151. [CrossRef]
7. Elchalakani, M.; Basarir, H.; Karrech, A. Green concrete with high-volume fly ash and slag with recycled aggregate and recycled water to build future sustainable cities. *J. Mater. Civ. Eng.* **2017**, *29*, 04016219. [CrossRef]
8. Aliabdo, A.A.; Abd Elmoaty, M.; Aboshama, A.Y. Utilization of waste glass powder in the production of cement and concrete. *Constr. Build. Mater.* **2016**, *124*, 866–877. [CrossRef]
9. Choi, S.; Lee, K.M. Influence of Na_2O content and Ms (SiO_2/Na_2O) of alkaline activator on workability and setting of alkali-activated slag paste. *Materials* **2019**, *12*, 2072. [CrossRef]
10. Shubbar, A.A.; Sadique, M.; Shanbara, H.K.; Hashim, K. The development of a new low carbon binder for construction as an alternative to cement. In *Advances in Sustainable Construction Materials and Geotechnical Engineering*; Springer: Singapore, 2020.
11. Grist, E.R.; Paine, K.A.; Heath, A.; Norman, J.; Pinder, H. The environmental credentials of hydraulic lime-pozzolan concretes. *J. Clean. Prod.* **2015**, *93*, 26–37. [CrossRef]
12. Zhang, J.; Shi, C.; Zhang, Z.; Ou, Z. Durability of alkali-activated materials in aggressive environments: A review on recent studies. *Constr. Build. Mater.* **2017**, *152*, 598–613. [CrossRef]
13. Collins, F.; Sanjayan, J.G. Cracking tendency of alkali-activated slag concrete subjected to restrained shrinkage. *Cem. Concr. Res.* **2000**, *30*, 791–798. [CrossRef]
14. Cartwright, C.; Rajabipour, F.; Radlińska, A. Shrinkage characteristics of alkali-activated slag cements. *J. Mater. Civ. Eng.* **2014**, *27*, B4014007. [CrossRef]
15. Collins, F.G.; Sanjayan, J.G. Workability and mechanical properties of alkali activated slag concrete. *Cem. Concr. Res.* **1999**, *29*, 455–458. [CrossRef]

16. Gu, Y.; Fang, Y. Shrinkage, Cracking, Shrinkage-Reducing and Toughening of Alkali-Activated Slag Cement—A Short Review. *J. Chin. Ceram. Soc.* **2012**, *40*, 76–84.
17. Bernal, S.A.; Provis, J.L. Durability of alkali-activated materials: Progress and perspectives. *J. Am. Ceram. Soc.* **2014**, *97*, 997–1008. [CrossRef]
18. Law, D.W.; Adam, A.A.; Molyneaux, T.K.; Patnaikuni, I. Durability assessment of alkali activated slag (AAS) concrete. *Mater. Struct.* **2012**, *45*, 1425–1437. [CrossRef]
19. Abolfathi, M.; Omur, T.; Kabay, N. Effect of microfibers or SRA on the shrinkage and mechanical properties of alkali activated slag/fly ash-based mortars incorporating recycled fine aggregate. *Constr. Build. Mater.* **2023**, *373*, 130883. [CrossRef]
20. Al Makhadmeh, W.; Soliman, A. On the mechanisms of shrinkage reducing admixture in alkali activated slag binders. *J. Build. Eng.* **2022**, *56*, 104812. [CrossRef]
21. Xu, R.; Kong, F.; Yang, R.; Wang, H.; Hong, T. Drying shrinkage mitigation of alkali-activated blast furnace slag-copper slag by polyether-based shrinkage reducing admixture and MgO-based expansion agent. *Constr. Build. Mater.* **2024**, *416*, 135172. [CrossRef]
22. Choi, S.; Ryu, G.S.; Koh, K.T.; An, G.H.; Kim, H.Y. Experimental study on the shrinkage behavior and mechanical properties of AAM mortar mixed with CSA expansive additive. *Materials* **2019**, *12*, 3312. [CrossRef] [PubMed]
23. Palacios, M.; Puertas, F. Effect of shrinkage-reducing admixtures on the properties of alkali-activated slag mortars and pastes. *Cem. Concr. Res.* **2007**, *37*, 691–702. [CrossRef]
24. *KS F 2563*; Ground Granulated Blast-Furnace Slag for Use in Concrete. Korean Standards: Seoul, Republic of Korea, 2019.
25. *KS L5405*; Fly Ash. Korean Standards: Seoul, Republic of Korea, 2018.
26. *ASTM C39/C39M-18*; Standard Test Method for Compressive Strength of Cylindrical Concrete Specimens. ASTM International: West Conshohocken, PA, USA, 2016.
27. *ASTM C469M-14*; Standard Test Method for Static Modulus of Elasticity and Poisson's Ratio of Concrete in Compression. ASTM International: West Conshohocken, PA, USA, 2014.
28. Ravikumar, D.; Neithalath, N. Reaction kinetics in sodium silicate powder and liquid activated slag binders evaluated using isothermal calorimetry. *Thermochim. Acta* **2012**, *546*, 32–43. [CrossRef]
29. Chang, J.J. A study on the setting characteristics of sodium silicate-activated slag pastes. *Cem. Concr. Res.* **2003**, *33*, 1005–1011. [CrossRef]
30. Shi, C.; Roy, D.; Krivenko, P. *Alkali-Activated Cements and Concretes*; CRC Press: Boca Raton, FL, USA, 2003.
31. Bílek, V.; Kalina, L.; Novotný, R.; Tkacz, J.; Pařízek, L. Some issues of shrinkage-reducing admixtures application in alkali-activated slag systems. *Materials* **2016**, *9*, 462. [CrossRef]
32. Nguyen, C.V.; Mangat, P.S.; Jones, G. Effect of shrinkage reducing admixture on the strength and shrinkage of alkali activated cementitious mortar. In *IOP Conference Series: Materials Science and Engineering*; IOP Publishing: Bristol, UK, 2018; Volume 371, p. 012022.
33. Jia, Z.; Yang, Y.; Yang, L.; Zhang, Y.; Sun, Z. Hydration products, internal relative humidity and drying shrinkage of alkali activated slag mortar with expansion agents. *Constr. Build. Mater.* **2018**, *158*, 198–207. [CrossRef]
34. Vakhshouri, B.; Nejadi, S. Empirical models and design codes in prediction of modulus of elasticity of concrete. *Front. Struct. Civ. Eng.* **2019**, *13*, 38–48. [CrossRef]
35. Zhan, P.M.; He, Z.H. Application of shrinkage reducing admixture in concrete: A review. *Constr. Build. Mater.* **2019**, *201*, 676–690. [CrossRef]
36. Das, B.B.; Kondraivendhan, B. Implication of pore size distribution parameters on compressive strength, permeability and hydraulic diffusivity of concrete. *Constr. Build. Mater.* **2012**, *28*, 382–386. [CrossRef]
37. Speziale, S.; Jiang, F.; Mao, Z.; Monteiro, P.J.; Wenk, H.R.; Duffy, T.S.; Schilling, F.R. Single-crystal elastic constants of natural ettringite. *Cem. Concr. Res.* **2008**, *38*, 885–889. [CrossRef]
38. Coppola, L.; Coffetti, D.; Crotti, E.; Candamano, S.; Crea, F.; Gazzaniga, G.; Pastore, T. The combined use of admixtures for shrinkage reduction in one-part alkali activated slag-based mortars and pastes. *Constr. Build. Mater.* **2020**, *248*, 118682. [CrossRef]
39. Hu, X.; Shi, C.; Zhang, Z.; Hu, Z. Autogenous and drying shrinkage of alkali-activated slag mortars. *J. Am. Ceram. Soc.* **2019**, *102*, 4963–4975. [CrossRef]
40. Maltese, C.; Pistolesi, C.; Lolli, A.; Bravo, A.; Cerulli, T.; Salvioni, D. Combined effect of expansive and shrinkage reducing admixtures to obtain stable and durable mortars. *Cem. Concr. Res.* **2005**, *35*, 2244–2251. [CrossRef]
41. He, Z.; Li, Z.J.; Chen, M.Z.; Liang, W.Q. Properties of shrinkage-reducing admixture-modified pastes and mortar. *Mater. Struct.* **2006**, *39*, 445–453. [CrossRef]
42. Semianiuk, V.; Tur, V.; Herrador, M.F. Early age strains and self-stresses of expansive concrete members under uniaxial restraint conditions. *Constr. Build. Mater.* **2017**, *131*, 39–49. [CrossRef]